

## Numerical Investigation of Reflection Properties of Fast and Slow Longitudinal Waves in Cancellous Bone: Variations with Boundary Medium

海綿骨中における高速波・低速波の反射に関する数値的検討：  
境界媒質による変化

Atsushi Hosokawa<sup>†</sup> (Dept. Elect. & Comp. Eng., Akashi Nat. Coll. Tech.)  
細川篤<sup>†</sup> (明石高専 電気情報)

### 1. Introduction

It has been shown that fast and slow longitudinal waves can propagate through *in vitro* cancellous bone.<sup>1</sup> In *in vivo* cancellous bone, the reflections of the fast and slow waves can be generated at the boundaries of cortical bone and bone marrow. Experimental approaches to clearly observe the ultrasound reflections appear to be difficult because the intensity of the reflected signals is very low owing to the ultrasound scattering attributed to the complex trabecular network. In such a case, numerical approaches, which generate no random noise, can be useful.

In this study, finite-difference time-domain (FDTD) simulations with microcomputed tomographic ( $\mu$ CT) models of bovine cancellous bone were performed to derive the reflection coefficients of the fast and slow waves. The variations in the reflection properties with the boundary medium were investigated.

### 2. Method

Cancellous bone models were reconstructed from three-dimensional (3D)  $\mu$ CT images of bovine femur. The thickness direction was determined to be parallel to the main orientation of the trabecular network in order to separately observe the fast and slow waves.<sup>1</sup> It was assumed that the pore spaces were completely filled with water. The schematic drawings of two simulation models are shown in **Fig. 1**. In this figure, (a) shows the cancellous bone model with an  $x\%$  ( $x = 100, 80, 60, 40, 20, 0$ ) bone layer, wherein twenty perfectly matched absorbing layers (PMLs)<sup>2</sup> were adopted at the opposite surface, and (b) shows the cancellous bone model with only the PMLs. The  $x\%$  bone represents a homogeneous bone with physical parameter values at a bone volume fraction of  $x\%$ .

Numerical simulations were performed using an elastic FDTD method.<sup>3</sup> The dimensions of the simulation models, including the water region, were  $16.53 \times 7.98 \times 7.98 \text{ mm}^3$  for the cancellous bone

model with the  $x\%$  bone layer and  $13.68 \times 7.98 \times 7.98 \text{ mm}^3$  for the model with only the PMLs. In these models, the spatial interval was  $57 \mu\text{m}$ . A transmitting area was set at a distance of  $7.98 \text{ mm}$  from the cancellous bone surface. A receiving area was set on the boundary surfaces between the cancellous bone and the  $x\%$  bone, and between the cancellous bone and the PMLs. The transmitting and receiving areas were flat circles with a diameter of  $3.99 \text{ mm}$ . The PMLs were set at all boundaries surrounding the simulation region. As the input, a single sinusoid at  $0.75 \text{ MHz}$  multiplied by a Hanning window was applied to the particle

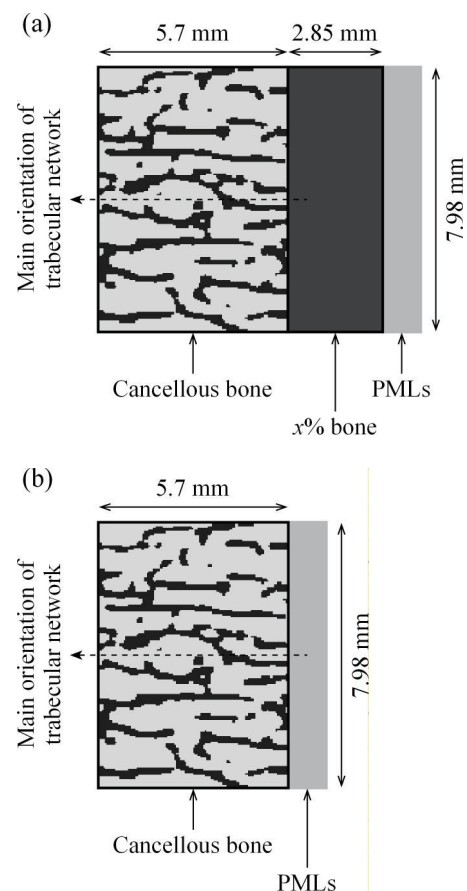


Fig. 1 Cancellous bone models (a) with an  $x\%$  bone layer and (b) with only PMLs.

displacement component at each point on the transmitting area. Its time interval was 4 ns. As the output, the sum of the normal stress components at all points on the receiving area was calculated.

In the case with the  $x\%$  bone layer, the fast and slow waves propagating in cancellous bone can reflect at the boundary. In the case with only the PMLs, no reflection can be generated. Therefore, only the reflected waveform can be calculated by subtracting the simulated waveform of the received signal in the latter case from that in the former case.<sup>4</sup>

### 3. Results and discussion

The simulated results for the reflection coefficients as a function of the cancellous bone porosity are shown in Fig. 2; (a) and (b) show the data of the fast and slow waves, respectively. At the porosities below 0.65, the small amplitude of the slow wave could not be measured. For the fast wave, the reflection coefficient values were positive at the boundaries of the 100% and 80% bone layers, but negative at the other boundaries. Moreover, the reflection coefficient at the 100% bone boundary increased with the porosity. As the density of the boundary layer decreased, the porosity dependence became weaker, and the reflection coefficient at the 0% bone boundary was almost constant. For the slow wave, at the 100% bone boundary, the reflection coefficient increased with the porosity but decreased at the other boundaries. Moreover, the reflection coefficient values at the 80% to 40% bone boundaries were large.

At the boundary in cancellous bone, both the fast and slow incident waves can be converted to both the fast and slow reflected waves.<sup>4</sup> The fast and slow waves can propagate mainly in the solid bone and the pore parts of cancellous bone, respectively.<sup>1</sup> Therefore, for the fast wave, the conversion to the slow wave can mainly arise at the high-density bone boundary, but the conversion to the fast wave can mainly arise at the low-density bone boundary. For the slow wave, the conversion to the slow wave can mainly arise at the high-density bone boundary, but the conversion to the fast wave can mainly arise at the low-density bone boundary. It is considered that the degrees of the conversions to the fast and slow waves can be associated with the reflection properties.

### 4. Conclusions

In this study, the variations in the reflection properties of the fast and slow waves with the boundary medium were observed. These variations can be associated with the conversions between the fast and slow waves at the boundary.

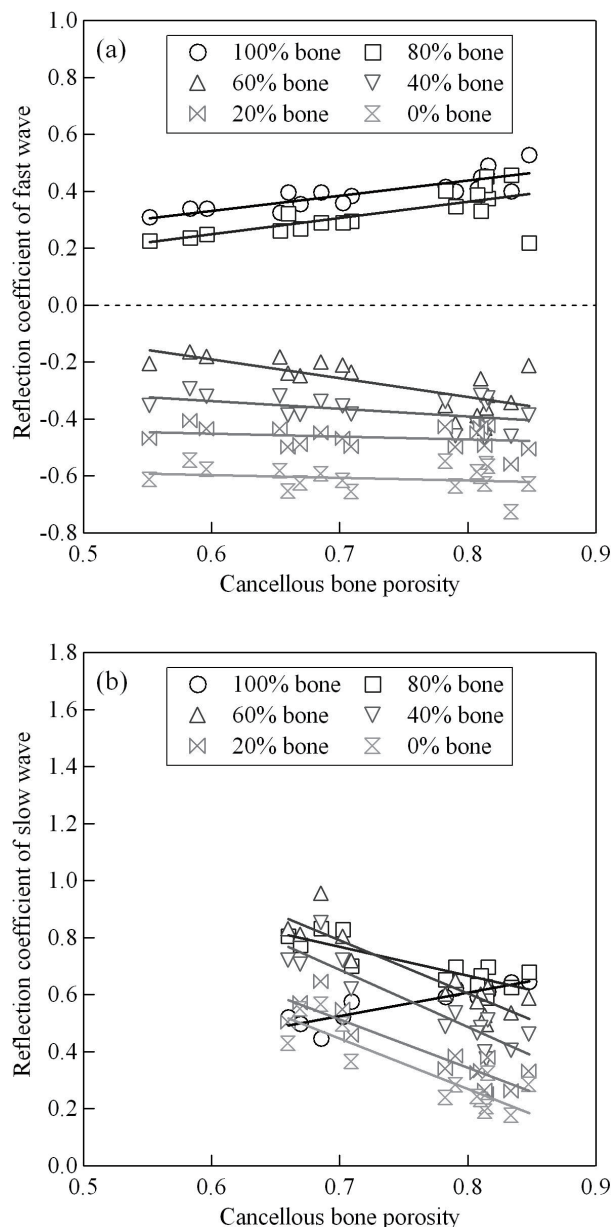


Fig. 2 Reflection coefficients of (a) fast and (b) slow waves in cancellous bone at the boundaries of  $x\%$  bone layers as a function of the cancellous bone porosity.

### Acknowledgment

Part of this study was supported by JSPS through a Grant-in-Aid for Scientific Research (B) (No. 24360161).

### References

1. A. Hosokawa and T. Otani: *J. Acoust. Soc. Am.* **101** (1997) 558.
2. W. C. Chew and Q. H. Liu: *J. Comput. Acoust.* **4** (1996) 341.
3. N. Endoh, *et al.*: *Jpn. J. Appl. Phys.* **44** (2005) 4598.
4. A. Hosokawa: *IEEE Trans. Ultrason. Ferroelectr. Freq. Control* **60** (2013) 1030.